larity index can be a powerful tool for systematizing the properties of chemical systems in a rigorous manner. Besides applications in drug design, the similarity index can be useful in correlating reactivities of functional groups in organic systems, in comparing similar molecules, in computerized interpretation of the IR spectra, and in pattern recognition.

Acknowledgment. This research was partially supported by the U.S. D.O.E. under contract DE-FC05-85ER250000 and by the Florida State University through time granted on its VAX and ETA10-G digital computers. One of the authors (J.C.) also acknowledges support by the Camille and Henry Dreyfus Foundation New Faculty Award Program.

Simulation of the Structure and Dynamics of the Bis(penicillamine) Enkephalin Zwitterion

Paul E. Smith, Liem X. Dang,† and B. Montgomery Pettitt*

Contribution from the Department of Chemistry, University of Houston, 4800 Calhoun Road, Houston, Texas 77204-5641. *Received April 16, 1990*

Abstract: We have performed a molecular dynamics simulation of the enkephalin derivative Tyr-(D)Pen-Gly-Phe-(D)Pen (DPDPE) in aqueous solvent. Electrostatic interactions were calculated with the Ewald method so as to accurately model the large interactions between the DPDPE zwitterion and the solvent and to avoid the use of electrostatic cutoff's or neutral chemical blocking groups. DPDPE is found to be extremely constrained with very little variation in the main-chain dihedral angles. Flexibility found in the region of the central glycine is greatly restricted compared with glycines in straight-chain peptides. Several conformational transitions are observed for the two aromatic side chains, indicating a high degree of flexibility in the side chains and that DPDPE does not have a single conformation in solution. This suggests that the arrangement of the tyrosine and phenylalanine aromatic residues in the bound conformation may be selected by the receptor environment. The main-chain conformation of DPDPE in solution has a parallel arrangement of peptide groups. This electrostatically unfavorable structure is stabilized by interactions of the carbonyls with the solvent. Solvent structure around the N terminus is found to be considerably localized, involving short ammonium cation to water contacts with lifetimes of the order of 50 ps or more. In comparison, water structure around the C terminus is much more mobile with lifetimes of the order of 20 ps or less.

I. Introduction

When studying the interactions between receptors and their ligands it is usual to have a reliable structure for both the receptor and the ligand. Without prior knowledge of at least one of these structures the possibility of isolating the major stabilizing interactions is considerably reduced if not impossible. Many systems of biochemical importance for which the structure or conformation of the receptor is unknown can be approached by using synthetically constrained ligands. One such system is that of the neurotransmitters and their interactions with the opioid receptors.[1]

Neurotransmitters are small peptides that facilitate the transfer of nerve impulses across the synaptic cleft. The initial nerve impulse along the neuron triggers the release of the neurotransmitters into the cleft where they diffuse toward a series of receptors on the opposite side of the cleft. The interaction between the neurotransmitter and the receptor enables the continuation of the nerve impulse. A wealth of information has been obtained on the action of different neurotransmitters with their respective receptors,[1,2] but very little structural detail is known. For opioids the problem is also compounded by the presence of more than one receptor type (δ, μ, and κ are known), each of which is specific for a different neurotransmitter or different conformations of the same neurotransmitter.

As the structure of the receptor sites is unknown the traditional approach to investigate the interactions between a receptor and a ligand is to search for common, and therefore important, structural features (pharmacophores) between known neurotransmitters.[3-5] This was attempted by starting with the two endogenous neuromodulators Tyr-Gly-Gly-Phe-Leu and Tyr-Gly-Gly-Phe-Met, known as Leu and Met enkephalin, respectively. By adding, deleting, and modifying various residues and then testing for biological activity, valuable information has been gained concerning the important features necessary for activity.[3] Most significantly, synthetic constraints were used to severely restrict the number of conformations available to the peptide at normal temperatures.

This type of mapping was used with some success and yielded the most specific and one of the most potent neurotransmitters known for the δ-opioid receptor.[3] This neurotransmitter is a pentapeptide enkephalin derivative with sequence Tyr-(D)Pen-Gly-Phe-(D)Pen (DPDPE). The penicillamine residue (an isopropylcysteine derivative) was used to constrain the ring structure via a disulfide bond.

DPDPE has been studied by NMR, model building, molecular mechanics, and quenched high-temperature molecular dynamics.[6] One major class of conformations was found to satisfy the experimental data but did not correspond to the lowest energy conformation using continuum solvent models. The search for a representative population distribution of conformers was hindered by the simplified treatment. Simulations under vacuum always gave structures with a strong interaction, or salt bridge, between the ammonium and carboxylate termini (unpublished results). This contradicted the available NMR evidence. On the other hand simulations using the dielectric constant of bulk water severely diminished all the electrostatic interactions, especially those with the ionic groups. Hence, the correct modeling of the solvent and

† Present address: IBM Research Labs, Almaden Research Center, 650 Harry Road, San Jose, CA 95120-6099.

(1) Schiller, P. W. In *Peptides: Analysis, Synthesis, Biology*, Volume 6, *Opioid Peptides: Biology, Chemistry, and Genetics*; Udenfriend, S.; Meienhofer, J., Eds.; Academic Press: New York, 1984; Vol. 6, pp 219-268.
(2) Hruby, V. J.; Krstenansky, J. L.; Cody, W. L. *Annu. Rep. Med. Chem.* **1984**, *19*, 303-312.
(3) Hruby, V. J.; Pettitt, B. M. In *Computer-Aided Drug Design: Methods and Applications*; Perun, T. J.; Propst, C. L., Eds.; Marcel Dekker: New York, 1989, pp 405-460.
(4) Mierke, D. F.; Said-Nejad, O. E.; Schiller, P. W.; Goodman, M. *Biopolymers* **1990**, *29*, 179-196.
(5) Aubry, A.; Birlirakis, N.; Sakarellos-Daitsiotis, M.; Sakarellos, C.; Marraud, M. *Biopolymers* **1989**, *28*, 27-40.
(6) Hruby, V. J.; Kao, L.; Pettitt, B. M.; Karplus, M. *J. Am. Chem. Soc.* **1988**, *110*, 3351-3359.

0002-7863/91/1513-67$02.50/0

the corresponding electrostatics, in particular the two ionic groups, will be important in obtaining any meaningful results.

The class of conformations that best fitted the NMR data displayed some interesting features.[6] The effect of cyclization and the use of the D-penicillamine residues (having transannular interactions) produced a very conformationally constrained molecule. The tyrosine and phenylalanine side chains adopted a folded form with a close arrangement of aromatic groups. In the literature there appears to be some confusion as to the exact arrangement of the tyrosine and phenylalanine aromatic groups required for specificity. Several crystal structures of enkephalins exist (see ref 5 and references therein) where the two aromatic groups adopt a variety of conformations even in the solid state. Both the folded[4] and extended[5] forms have been proposed for δ opioid activity.

There is also a rather unusual proposed[6] arrangement of amide groups within the cyclic structure of the peptide. Three of the amide groups in the macrocycle (between residues (D)Pen-Gly, Gly-Phe, and Phe-(D)Pen) are aligned so that their NH groups are pointing toward the aromatics, with their CO groups pointing in the opposite direction, to give an amphiphilic type of structure.[3] This parallel arrangement of peptide dipoles would not be expected to be the most energetically favorable although previous continuum solvent models suggest this arrangement is quite stable.[6]

With all these factors in mind we have used the molecular dynamics technique with an Ewald[7,8] treatment of the electrostatics to simulate DPDPE in explicit solvent. Of particular interest were the interactions between the two ionic groups and the two ionic groups with water and the general flexibility or rigidity of the molecule. So as to represent the solvation characteristics more rigorously special attention has been paid to the calculation of electrostatic interactions. As well as providing more insight into the solvation of zwitterion peptides in solution the results may aid in the design of yet more potent and specific neurotransmitters.

Molecular dynamics has been used to study the properties of the natural enkephalins and several enkephalin derivatives. Mierke et al.[4] studied several enkephalin derivatives where phenylalanine was replaced by β-naphthylalanine. The preference for μ selectivity was related to the extended structure as determined by NMR and molecular dynamics calculations. Correspondingly δ selectivity was related to a more closely packed arrangement of the aromatic side chains. This is in agreement with the folded structure previously predicted for DPDPE.[6]

Yoneda et al.[9] studied Met enkephalin and the Met enkephalin dimer solvated by a sphere of water. They found the monomer existed in several different conformations in solution. One of the major conformations of the monomer involved a head-to-tail salt bridge between the zwitterion termini. This type of conformation has since been excluded on the basis of results from recent NMR experiments.[10] Again, this illustrates the care that must be taken when modeling ionic groups even in explicit solvent.

II. Method

DPDPE was simulated with 429 waters in a cubic box of length 24.17 Å with periodic boundary conditions. The system was simulated for a total of 250 ps, in the NVE ensemble, with a resulting average temperature of 316 K. The force field incorporated the latest OPLS[11] nonbonded parameters in combination with the CHARMM[12] bonded parameters. Only polar hydrogens were included, and a conservative time step of 0.5 fs was used throughout. We used a modified SPC parameter set developed for flexible water to model the solvent.[13]

All electrostatic interactions were calculated with the Ewald procedure tabulated on a 50 × 50 × 50 lookup grid. In the Ewald procedure no electrostatic cutoff distances are used and so all $N(N-1)/2$ nonbonded interactions are calculated at each time step. The initial conformation for DPDPE was taken from previous studies.[6] Initial velocities were assigned from a Maxwell–Boltzmann distribution at 300 K. The system was allowed to evolve for 50 ps with intermitant scaling of velocities. At this point the system was found to be equilibrated by inspection of mechanical averages and energy fluctuations. A simulation of 200 ps was then performed, without further velocity scaling. The results are analyzed below.

During our initial runs we observed that the carboxylate terminus was distorted by a strong ionic coupling between one of the carboxylate oxygens and the NH group of (D)Pen-5 (distance 1.2 Å). This interaction was so strong that the N–C_α–C angle was decreased to 90°. The problem seemed to arise because the OPLS force field, which has been developed for Monte Carlo simulations using rigid bonds and angles, has no VDW's repulsion between atom pairs when one of the atoms is a hydrogen. Normally a reasonable hydrogen contact distance is maintained by the VDW's interaction with the nitrogen of the NH group. In our case this is a 1,4 interaction which the OPLS set divides by a factor of 8.0.[11] It appears that this scaling reduces the repulsion between the carboxylate oxygen and the nitrogen, resulting in an unreasonably short interatomic distance. To overcome this problem we did not scale the 1,4-VDW's interaction between the carboxylate oxygens and the nitrogen of (D)Pen-5.

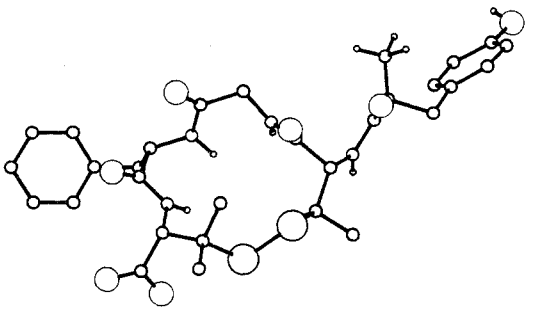

Figure 1. Structure of DPDPE after 50 ps of equilibration.

Table I. Average and RMS Fluctuations of Energies[a]

energy	av	RMS
potential	−46051	100
kinetic	5270	95
DPDPE kinetic	205	24
water kinetic	5065	94
DPDPE potential	−215	46
water potential	−47124	148
water internal	2990	108
DPDPE–water potential	−1703	87
DPDPE bond	77	15
DPDPE angle	92	16
DPDPE dihedral	40	9
DPDPE imp-dihedral	30	9
DPDPE VDW's	−21	9
DPDPE electrostatic	−432	44
end-to-end distance	13.13	0.56

[a] Energies in kJ mol^{-1}, distances in Å.

III. Results and Discussion

(a) Dynamics of DPDPE. The initial conformation for DPDPE was taken from previous studies that used NMR derived coupling constants and interatomic distance constraints together with molecular mechanics and molecular dynamics calculations.[6] However, during the equilibration period χ^1 of tyrosine flipped from the initial t conformation to a g^- conformation. The side chain remained in this conformation for the remainder of the simulation. Hence the conformation at the start of the analysis (50 ps) was not the same as that at the start of the simulation (0 ps). As the new conformation did not violate any of the NMR constraints we continued the simulation with DPDPE in the new conformation. The new conformation is shown in Figure 1. Furthermore, subsequent to our simulation Milon et al.[14] found

(7) Ewald, P. *Ann. Phys.* **1921**, *64*, 253–287.
(8) de Leeuw, S. W.; Perram, J. W.; Smith, E. R. *Proc. R. Soc. London A* **1980**, *373*, 27–56.
(9) Yoneda, S.; Kitamura, K.; Doi, M.; Inoue, M.; Ishida, T. *FEBS Lett.* **1988**, *239*, 271–275.
(10) Karayannis, T.; Gerothanassiss, I. P.; Sakarellos-Daitsiotis, M.; Sakarellos, C.; Marraud, M. *Biopolymers* **1990**, *29*, 423–439.
(11) Jorgensen, W. L.; Tirado-Rives, J. *J. Am. Chem. Soc.* **1988**, *110*, 1657–1666.
(12) Brooks, B. R.; Bruccoleri, R. E.; Olafson, B. D.; States, D. J.; Swaminathan, S.; Karplus, M. *J. Comput. Chem.* **1983**, *4*, 187–217.
(13) Dang, L. X.; Pettitt, B. M. *J. Phys. Chem.* **1987**, *91*, 3349–3354.
(14) Milon, A.; Miyazawa, T.; Higashijima, T. *Biochemistry* **1990**, *29*, 65–75.

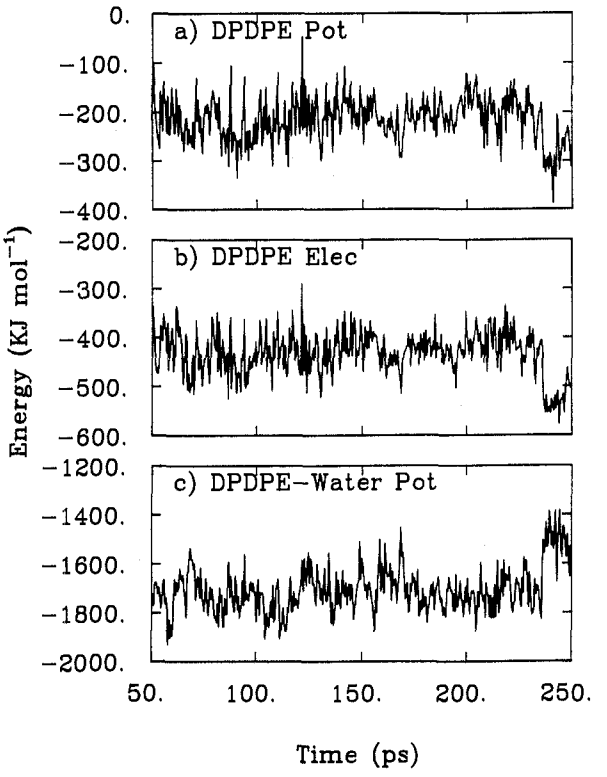

Figure 2. Time histories of the (a) DPDPE potential energy, (b) DPDPE electrostatic energy, and (c) DPDPE–water potential energy.

that the conformation of several enkephalin derivatives when bound to a membrane did not include a membrane-bound tyrosine ring (the tyrosine residue is required for activity).[3] Assuming that the membrane and receptor bound conformations are the same,[14] or at least similar, a close packing of the phenylalanine and tyrosine rings is not necessarily required for the active conformation.

Table I shows the averages and rms deviations for various energy terms over the 200 ps of production. The total potential energy found for the water–water interactions is a direct result of the Ewald treatment of the electrostatic interactions which effectively includes interactions between atom *i* and atom *j*, and also atom *i* and all the periodic images of atom *j*. A small drift in the total energy is associated with the use of a grid lookup procedure giving rise to small errors in the force calculation which can only be removed by using a finer grid. Due to computational limitations, this is not always possible. We found an energy drift of approximately 1 kJ mol^{-1} ps^{-1} out of a total energy of 10^5 kJ mol^{-1}. The magnitude of the energy drift is reasonable for this type of calculation.

Figure 2a shows the time history of the DPDPE potential energy. The intramolecular potential energy fluctuated about an average value of −215 kJ mol^{-1} until 235 ps into the simulation when the potential energy changed abruptly. This coincided with a lowering of the DPDPE electrostatic energy (Figure 2b) and a corresponding rise in the DPDPE–water potential energy (Figure 2c). All three changes were related to a conformational change in the peptide. At approximately 235 ps the peptide group between D-penicillamine and glycine underwent a full 180° flip by simultaneous rotation of the ψ_2 and ϕ_3 dihedral angles. This is illustrated in Figure 3 which shows the time histories of the important dihedral angles in DPDPE. The above amide flip (see ψ_2 in Figure 3c and ϕ_3 in Figure 3d) produced a conformation that was electrostatically more favorable with respect to the rest of the DPDPE molecule (Figure 2a) but unfavorable with respect to the DPDPE–water potential (Figure 2c). The new conformation has a γ turn involving residues (D)Pen-2, Gly, and Phe with a hydrogen bond between the carbonyl oxygen of (D)Pen-2 and the amide hydrogen of Phe. This is the only intramolecular hydrogen bond found during the whole simulation. All other polar groups only hydrogen bond to solvent molecules. This new conformation

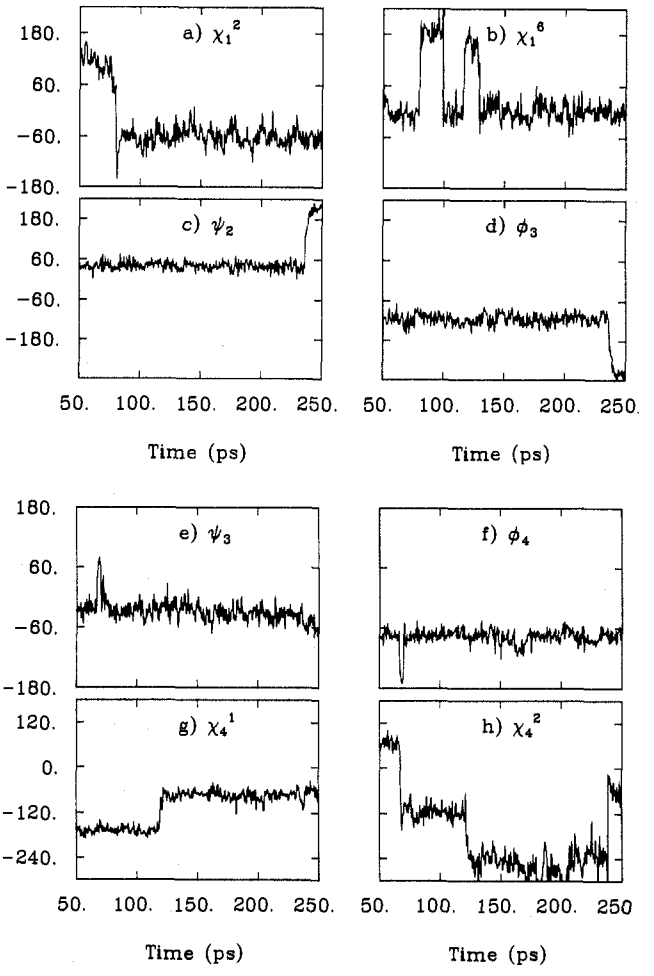

Figure 3. Time histories of several DPDPE dihedrals.

Table II. Initial, Final, Average, and RMS Fluctuations for the Dihedrals

dihedral	initial (0 ps)[a]	start (50 ps)	finish (250 ps)	av	RMS
ψ_1	163	152	168	146	17
χ_1^1	−163	−57	−72	−70	12
χ_1^2	51	123	−107	−37	51
χ_1^6	−179	26	12	28	64
ϕ_2	111	66	85	79	14
ψ_2	13	31	−147	51	37
χ_2^1	180	178	−177	173	9
χ_2^2	143	129	122	140	15
χ_2^3	−110	−131	−162	−121	13
ϕ_3	−98	−103	91	−124	38
ψ_3	−18	−28	−62	−30	18
ϕ_4	−72	−80	−90	−77	17
ψ_4	−46	−52	−28	−44	17
χ_4^1	179	−152	−80	−107	28
χ_4^2	68	55	−89	−176	85
ϕ_5	83	102	90	93	13
ψ_5	56	66	54	52	15
χ_5^1	−70	−54	−47	−64	12
χ_5^2	119	141	123	124	16

[a] See ref 6.

persists for at least 15 ps even though the initial conformation is unfavorable with respect to the surrounding solvent. It appears that for most of the simulation the parallel arrangement of peptide dipoles was significantly stabilized by interactions with the surrounding solvent; however, clearly other conformations of the main chain are possible.

Table II shows the averages and rms deviations of the important dihedrals in DPDPE. Analysis of the dihedrals and dihedral averages in terms of NMR coupling constants will be presented in a future publication.[15] Except for the side-chain dihedrals and

the main-chain dihedrals ψ_2 and ϕ_3, the rms fluctuations were very small illustrating the rigidity of the cyclic structure.

The final conformation of both the tyrosine and phenylalanine rings did not correspond to that of the initial (0 ps) structure. The final conformation had a more extended structure with both rings surrounded by bulk solvent. Normally, this would be an unfavorable situation for the hydrophobic aromatic groups, and we would not expect this conformation to be stable over a long period of time.

The tyrosine ψ and χ^1 dihedrals (Table II) did not vary considerably from their values after equilibration. However, we did observe some dihedral transitions that involved tyrosine ring rotations. The first at 80 ps was attributed to a phenyl ring rotation around χ^2 but without rotation of the tyrosine hydroxyl group, i.e. a rotation about the C_γ–C_ζ axis (Figure 3a). At 100, 115, and 130 ps the hydroxyl proton rotated by 180° (Figure 3b).

It is interesting to note that due to the cyclic nature of DPDPE, and the rigidity of the amide bond, a peptide group can only rotate via the correlated motion of the two dihedrals on either side of it. This process occurred twice during the simulation: the case we mentioned previously (involving rotation around ψ_2 and ϕ_3) and after 70 ps for rotation around ψ_3 and ϕ_4 (Figure 3, parts e and f). Both amide flips involved the central glycine residue which is the most conformationally flexible residue. The second amide flip was short lived and accompanied by phenyl ring rotation around χ^2 of phenylalanine (Figure 3h). It also lowered the peptide potential energy and was unfavorable in terms of the solvation energy which, in part, drives the system out of this configuration. This concerted motion preceeded rotation of the phenyl ring which forced the peptide bond between glycine and phenylalanine to rotate out of the way. After the phenyl ring rotated through 180° the peptide bond then flipped back to its original orientation. It seems that phenyl ring rotation might be significantly hindered by the presence of the peptide group. The phenyl ring of phenylalanine rotated a second time at 240 ps without a corresponding peptide flip, but in this case the conformation of the side chain had changed dramatically (due to a rotation around χ^1 of phenylalanine from the t conformation to the g^- conformation at 120 ps, Figure 3g) and rotation could then occur without the concerted motion of the peptide group. This latter conformational change was also accompanied by phenyl ring rotation.

It should be noted that recent experimental evidence suggests that the tyrosine χ^1 adopts a trans conformation.[16] In this study both the t and g^- were observed. However, in this case as well as in the change of the macrocycle (Figure 3) far too few events were observed to interpret this as representative of equilibrium behavior for the conformational population distribution functions. These events are only representative of possibilities not probabilities in solution.

Most of the transitions observed involved only side-chain atoms. The main-chain dihedrals, including the glycine residue, were remarkably rigid and result in a well-defined and constrained cyclic structure. The rigidity of the central glycine residue has been noted before and used to explain the separation of the two glycine H_α protons in the NMR spectrum of DPDPE.[6] The region around glycine could be made more rigid by replacing glycine with alanine, or some other small amino acid. Unfortunately, substitution for alanine or D-alanine results in significant loss in biological activity.[3] At present it appears that the three amide groups are not constrained to have the same orientation but do yield the same orientation when averaged over time.

(b) Zwitterionic Solvation Properties. One of the major aims of this work is to obtain valuable information concerning the properties and dynamics of zwitterions in solution. As most peptides exist as zwitterions in solution near physiological conditions, characterization of their solvation and its effect on solution properties of peptides is of great interest.

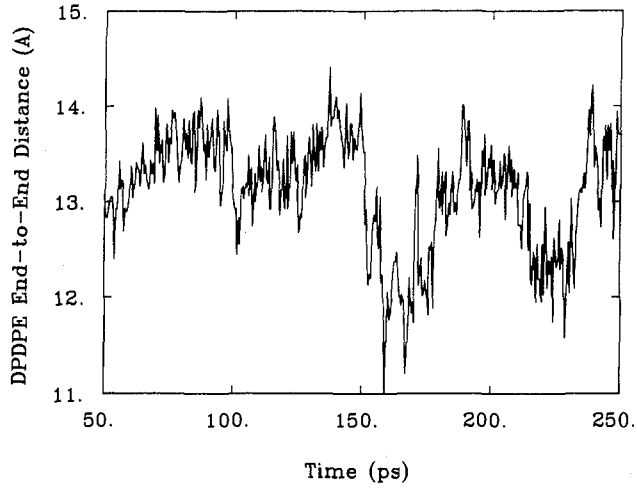

Figure 4. Time history of the DPDPE end-to-end distance.

As mentioned previously treatment of zwitterions by a continuum dielectric or the use of neutral blocking groups proved troublesome and prompted the work presented here. In order to treat the DPDPE zwitterion more accurately we used the Ewald method to correctly calculate electrostatic effects without the need for truncation techniques. We also used a flexible water model to accurately represent the solvent dynamics and any corresponding energy exchanges between the solvent and the peptide. Some of the results obtained for the DPDPE zwitterion are characteristic of zwitterions in general.

In Table I we gave the average and rms deviation for the end-to-end distance (taken to be the NH_3^+ to CO_2^- distance) in DPDPE. Figure 4 shows the fluctuations in end-to-end distance as a function of time. As shown in the figure, the end-to-end distance fluctuated between a minimum of 11.0 Å and a maximum of 14.5 Å. There appeared to be some oscillatory motion with a period of approximately 100 ps. Another interesting feature is the sharp reduction of overall length in the 150-ps region. We attribute this change in length to the global flexibility of the peptide as there were no dihedral transitions within this time regime. What we can say with confidence is that, in contrast to the vacuum calculations, the two ionic groups did not appear to irreversibly diffuse toward each other. The difference between these results and the previous calculations can be explained by considering the solvation shells surrounding both ionic groups (see later), which increase the effective size of both groups sustaining a significant separation distance. The observed separation of the zwitterionic centers is in accord with experimental NMR evidence for Leu enkephalin.[10]

The fluctuations in the DPDPE end-to-end distance have also been analyzed by calculating the power spectrum for the above time series (not shown). This spectrum gives peaks at frequencies of 0.02, 0.03, and 0.12 ps^{-1}. These three frequencies were also observed for the radius of gyration in a recent simulation of metmyoglobin in aqueous solution.[17] This suggests that the periods of oscillation observed for the end-to-end distance in DPDPE are quite possibly due to variations in the surrounding solvent structure which force the peptide to compress and expand on the same time scale as for metmyoglobin.

To investigate the structure of water around the two ionic groups we have calculated the relevant radial distribution functions, $g(r)$. Figure 5a shows the calculated g_{OO}, g_{OH}, and g_{HH} for water from our simulation. Figure 5, parts b and c, shows the radial distribution functions between N^+ and water oxygen and hydrogen, and O^- and water oxygen and hydrogen. The fact that $g(r)$ for these latter species pairs only approaches unity at large distances (>10 Å) is a consequence of the physical shielding that occurs

(15) Al-Obeidi, F.; Smith, P. E.; Pettitt, B. M. In preparation.
(16) Mosberg, H. I.; Sobczyk-Kojiro, K.; Subramanian, P.; Crippen, G. M.; Ramalingam, K.; Woodward, R. W. *J. Am. Chem. Soc.* **1990**, *112*, 822–829.
(17) Findsen, L. A.; Subramanian, S.; Pettitt, B. M. *Biophys. J.* Submitted.

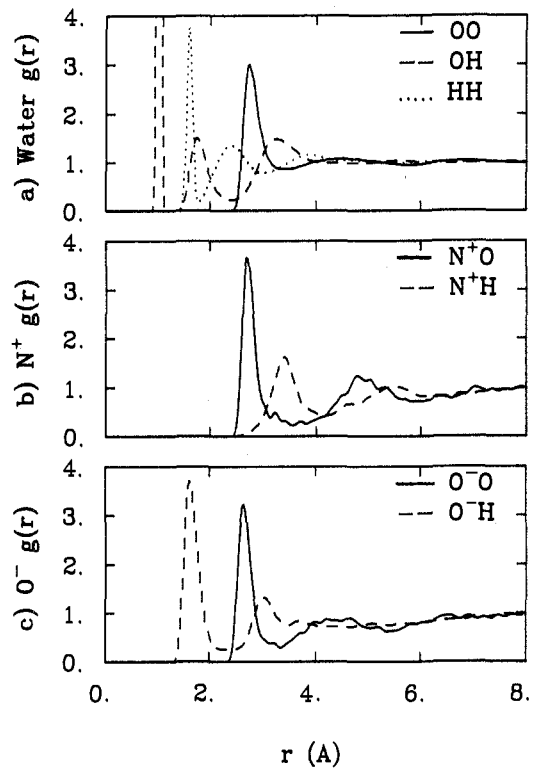

Figure 5. Radial distribution functions calculated for (a) water, (b) N^+, and (c) O^- termini of DPDPE.

Table III. Radial Distribution Functions

$g(r)$	peak positions	integrated to	coordination no
water O–O	2.75	3.23	3.9
water O–H	1.02, 1.76	1.22, 2.43	2.0, 3.8
water H–H	1.60, 2.40	1.79, 2.98	1.0, 6.2
DPDPE N^+–O	2.69	3.52	3.8
DPDPE N^+–H	3.42	4.10	9.8
DPDPE O^-–O	2.62	3.30	3.2
DPDPE O^-–H	1.60, 3.04	2.37	3.0

due to the peptides excluded volume. The results are summarized in Table III.

The results in Figure 5a for bulk waters agree well with previous calculations.[13] Comparison of g_{OH} for water and g_{O^-H} for carboxylate oxygen to water hydrogen shows that the first coordination shell occurred at smaller interatomic distances in the anion case (r = 1.76 and 1.60 Å, respectively). This is to be expected due to the higher magnitude of charge found on a carboxylate oxygen as opposed to an amide oxygen (−0.8 vs −0.5 electron units for the OPLS force field). We have also integrated $g(r)$ in the first solvation shell to yield the coordination number for a specific atom. Integration of the first peak in the water g_{OO} (3.23 Å) results in an average of 3.9, i.e. 4, oxygen atoms in the first solvation shell, and integration past the first two peaks in the water g_{OH} (2.43 Å) gives 3.8, i.e. 4, hydrogen atoms in the first solvation shell (of which, two of the hydrogens are bonded to the oxygen). In the case of the carboxylate anion the coordination numbers of both oxygen and hydrogen are found to be 3.2 and 3.0, respectively. These results compare well with Monte Carlo simulations of ammonium and carboxylate groups in water where coordination numbers of 3.4 for both oxygen and hydrogen were found.[18]

For the ammonium cation the first solvation shell was also closer to the charged nitrogen atom compared with the first water solvation shell (2.69 and 2.75 Å, respectively). The number of oxygens found in the first solvation shell of the nitrogen atom (<3.52 Å) corresponded to almost four water molecules per nitrogen atom (see Table III). Closer examination of the dynamics trajectories shows that three of these water molecules were bonded to the three NH groups with a fourth water molecule located slightly further away.

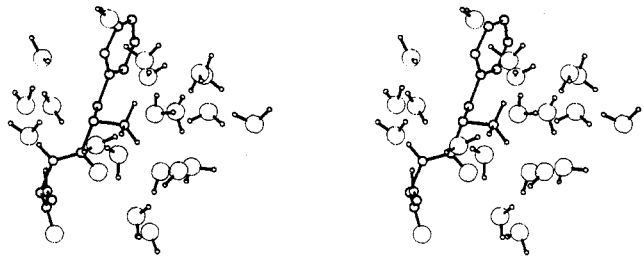

Figure 6. Stereoview of the solvation of the ammonium terminus by water. All atoms within 8.0 Å of the terminal nitrogen atom are shown. Note that there is a water oxygen directed toward each of the hydrogen atoms.

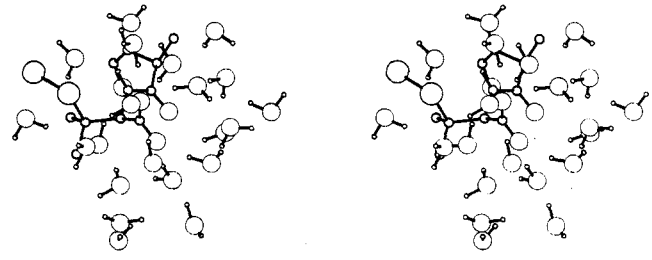

Figure 7. Stereoview of the solvation of the carboxylate terminus by water. All atoms within 8.0 Å of the terminal carbon atom are shown. Note that there are three water hydrogens directed toward each of the oxygen atoms.

Figures 6 and 7 are stereoviews of a dynamics snapshot showing the instantaneous structure of water surrounding the ammonium and carboxylate groups, respectively. In the case of the ammonium cation (Figure 6) each hydrogen can be seen to be hydrogen bonded to a single water oxygen atom. The fourth water molecule in the first solvation shell is located at a slightly larger distance from the cation center. Figure 7 illustrates the solvent structure around the carboxylate group. Each of the carboxylate oxygens is hydrogen bonded to three hydrogens from different water molecules. The carboxylate oxygens display tetrahedral coordination in this case. This explains the higher number of water molecules in the first solvation shell of the carboxylate group compared to the ammonium group.

Figure 8 shows the time series for the ammonium nitrogen to water oxygen distance for several different water molecules. Three water molecules (W162, W275, and W306) remained tightly bound to the ammonium group at an average distance of 2.75 Å, with small magnitudes of oscillation (rms 0.14 Å), for over 45 ps. The average distance of separation compared well with the position of the first peak in g_{N^+O} at 2.69 Å. After 245 ps water W275 (Figure 8c) was replaced by the incoming W117 (Figure 8a). This illustrates that the ammonium cation tightly binds, or is tightly solvated by, three water molecules that remain in contact with the cation center for periods of 50 ps or more. This strong solvation will increase the effective size of the group, and any motion of the group will therefore include the bound water molecules or result in the breakage of some hydrogen bonds to the solvent. These observations should also be relevant for solvated lysine side chains in protein structures.

Figure 9 shows the distance time series to the two carboxylate oxygen atoms. The average oxygen-to-oxygen distance for bound water molecules was 2.69 Å with an rms deviation of 0.16 Å. This also compared well with the position of the first peak in g_{O-O} at 2.62 Å. It is immediately obvious that water does not bind as tightly to the carboxylate group, with water molecules staying in close contact with the carboxylate oxygens for an average of only 20 ps. The figures show both arrival and departure of water molecules from bulk solution. Only one water molecule (W163) remained bound to a carboxylate oxygen for the whole 50 ps shown

(18) Jorgensen, W. L.; Gao, J. *J. Phys. Chem.* **1986**, *90*, 2174–2182.

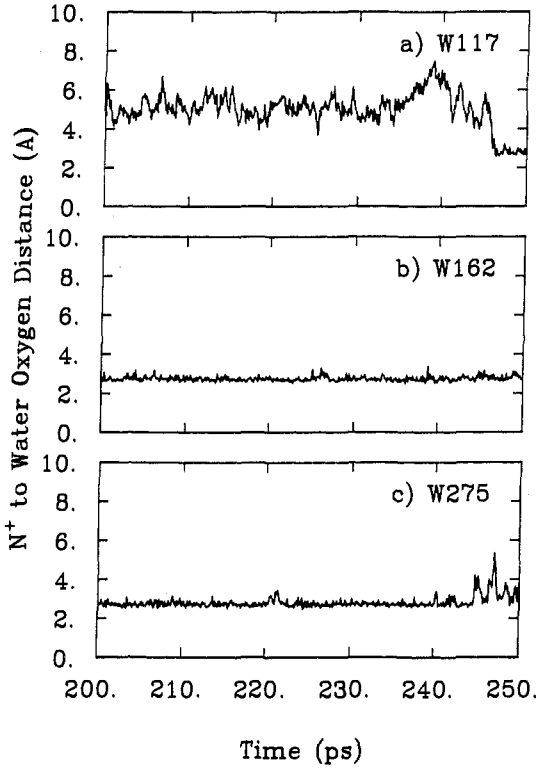

Figure 8. Time histories of the distance between N^+ and water oxygen for selected water molecules.

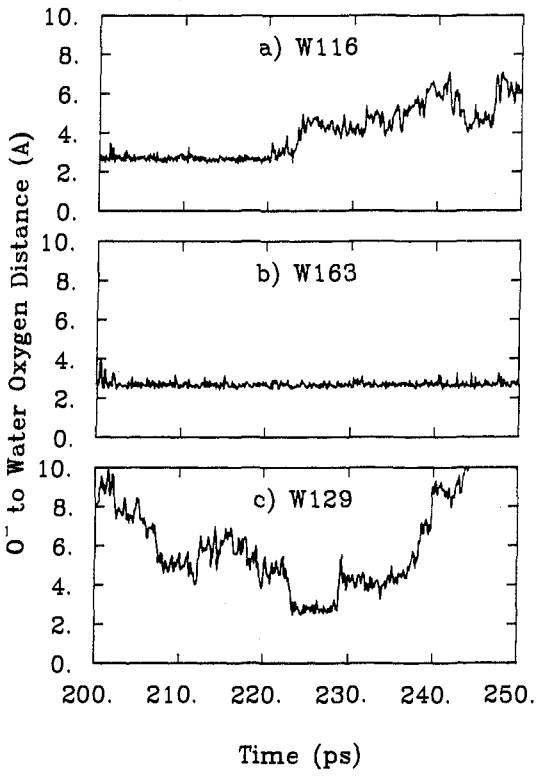

Figure 9. Time histories of the distance between O^- and water oxygen for selected water molecules.

here. In the case of water W163 there was a secondary interaction with the NH of (D)Pen-5 that appeared to stabilize the O–W163 interaction. Although this interaction was not a direct hydrogen bond it certainly restricted the motion of W163. We also found that both waters W78 and W116 bound to one oxygen and then switched to bind to the other oxygen. The differences we have found for the solvent mobilities and structure around the ammonium and carboxylate groups will be important in analyses of their dynamics.

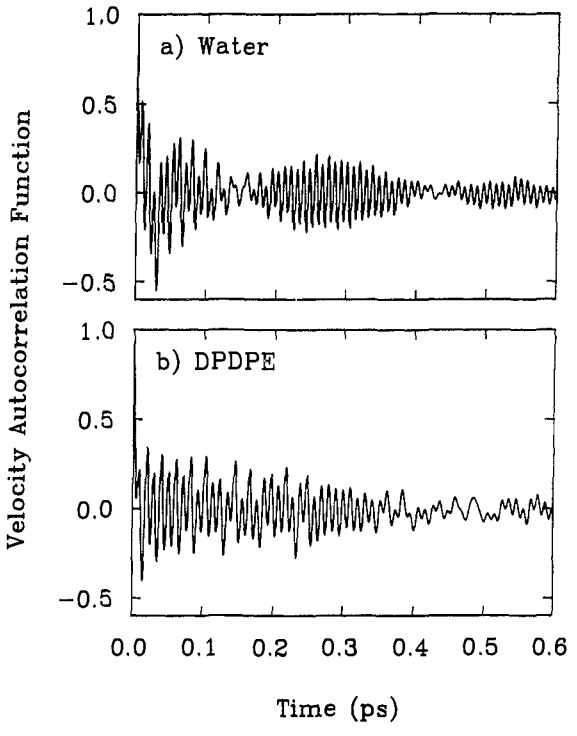

Figure 10. Calculated velocity autocorrelation function for (a) water and (b) DPDPE.

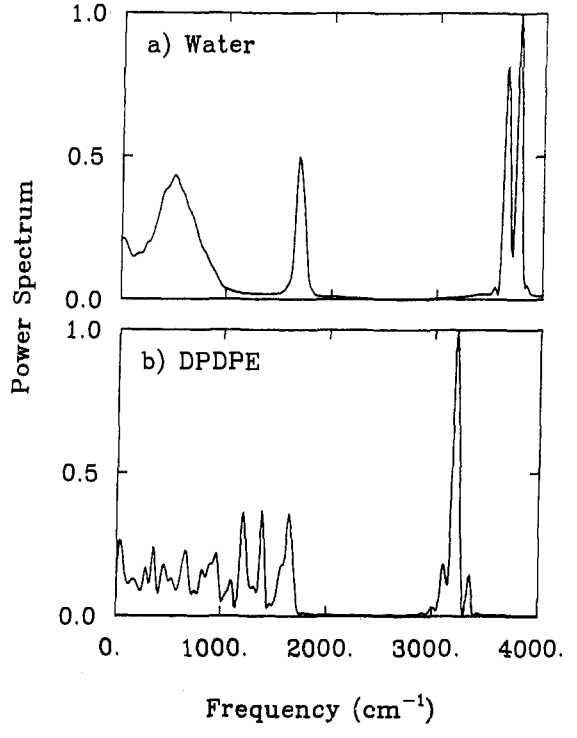

Figure 11. Calculated power spectrum of the velocity autocorrelation function for (a) water and (b) DPDPE.

(c) Time Correlation Functions. Time correlation functions have been used as a sensitive indicator of solvated peptide dynamics since the first peptide solvation simulation was performed.[19] One of the more interesting features of the simulation was the velocity autocorrelation function (VACF) of water. This is shown in Figure 10a, with the corresponding power spectrum shown in

(19) Rossky, P. J.; Karplus, M. *J. Am. Chem. Soc.* **1979**, *101*, 1913–1937.

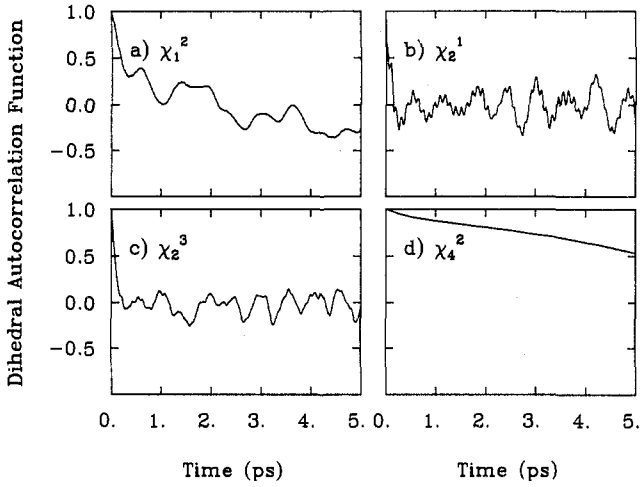

Figure 12. Calculated dihedral autocorrelation functions for several dihedrals in DPDPE.

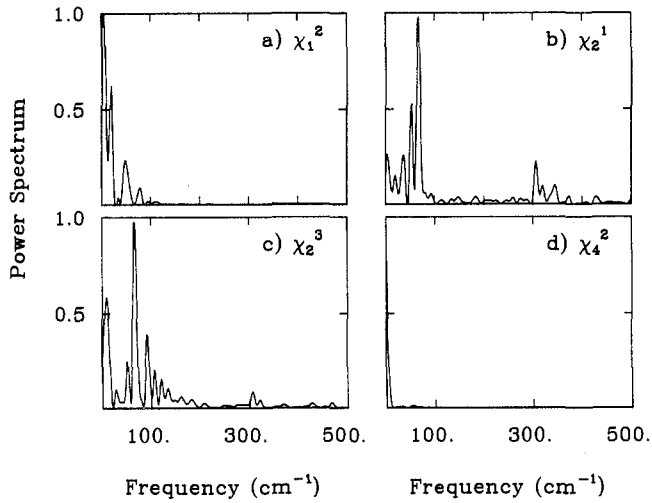

Figure 13. Calculated power spectrum of the dihedral autocorrelation function for several dihedrals in DPDPE.

Figure 11a. Both will be discussed together. As our model for water was flexible and therefore included all internal vibrational modes these will appear in the VACF and power spectrum. The power spectrum for water has two resolved high-frequency peaks that correspond to the asymmetric and symmetric O–H stretching frequencies (3644 and 3774 cm^{-1}, respectively). In the VACF these two frequencies appear as a high-frequency oscillation of period 0.05 ps. The small separation between the two peaks is responsible for the beat pattern observed in the VACF. The frequency of the beat pattern corresponds to the frequency difference between the two high-frequency components. In our case this is 130 cm^{-1}, or 3.9 ps^{-1}, which corresponds to a period of 0.3 ps. The other distinctive peak in the power spectrum is found at 1670 cm^{-1} and is associated with the water-bending mode. The broad low-frequency peak below 1000 cm^{-1} describes fluctuations in the gross solvent structure.

It should be noted that these calculations for the VACF of water are an improvement over previous results from this laboratory.[13] In the present case the two high-frequency peaks are well resolved in the power spectrum. This is most probably due to the considerably longer simulation times used for our system. Although we have a peptide zwitterion in the center of our system this should only have a minor effect on the results for pure water due to the relatively small percentage of water in contact with peptide atoms.

Figures 10b and 11b show the VACF and corresponding power spectrum for the atoms of DPDPE. The power spectrum shows a high-frequency peak at 3200 cm^{-1} which corresponds to the N–H stretching mode. This frequency is also apparent in the VACF. The peak at 1640 cm^{-1} can be assigned to the carbonyl stretch of the amide groups. While there is little overlap in frequency between the NH and OH oscillators there is considerable overlap between the water-bending motions near 1670 cm^{-1} and the carbonyl stretch at 1640 cm^{-1}. Such a strong overlap is important in allowing energy flow between solvent and solute. The remaining peaks in the DPDPE power spectrum represent various bending and flexing motions that are not simply characterizable. However, it is clear that there is a large spectral overlap from 0 to 1700 cm^{-1} between the solvent and solute enabling facile energy transfer over a wide variety of frequencies.

We have also computed the dihedral autocorrelation functions (DACF) for the important dihedrals in DPDPE. A sample of these are shown in Figure 12 together with their power spectra in Figure 13. The DACF's of the constrained main chain dihedrals generally decay very quickly within 0.5 ps. The more flexible side-chain dihedrals, in particular χ^2, have much more slowly decaying correlation functions. Indeed, the DACF of Phe-2 χ^2 has an extremely slow decay (Figure 12d). This high degree of correlation is representative of slow diffusive behavior and the correspondingly slow loss of memory.

Some fine structure, in the form of high-frequency oscillations, is also observed for several of the dihedrals (see Figure 12b). In the case of (D)Pen-2 χ^1 this appears as a peak at 310 cm^{-1} in the corresponding power spectrum which is near the libration or cage-rattling frequency of water. The power spectra of (D)Pen-2 χ^1 and χ^3 (Figure 13, spectra b and c, respectively) show that they display similar time dependence of motion as both have peaks at around 70 cm^{-1}. This could be indicative of a crankshaft motion of the disulfide bond as previously observed in continuum simulations.[3,6] This type of motion gave rise to the only mode that was stronger than the zero-frequency modes.

IV. Conclusions

The general overall structure of DPDPE in solution was consistent with a constrained cyclic structure with little flexibility in the main-chain dihedrals. The relative orientation of the tyrosine and phenylalanine aromatic rings was not restricted to one conformation suggesting an environmentally induced fit of the side chains on binding to the δ receptor. The most flexible parts of the main chain were located around the central glycine. Assuming that the more constrained a structure is the less entropy loss occurs on binding to the receptor (given that it is constrained to a conformation that is recognized by the receptor), then constraining the dihedrals around glycine could be of great significance. As simple substitution results in reduced activity some other synthetic modification of glycine would have to be achieved. This type of derivative might also restrict the peptide groups to be aligned and thereby prove if alignment is required or desirable for binding or specificity. Alignment of the peptide dipoles may play a very important role in the observed specificity for DPDPE if the side chains are as flexible as found in this work.

The simulation in explicit solvent with a flexible water model and careful treatment of electrostatic interactions gave a more satisfactory description of the dynamics of the DPDPE zwitterion. The ionic groups did not diffuse toward each other because their separation appeared to be maintained by the interactions between the solvent shells surrounding each ion. The parallel arrangement of peptide dipoles found in previous studies is more readily explained by invoking stabilizing interactions with the surrounding solvent. While this simulation was not long enough to produce reliable population distributions of the conformational states, it is clear that considerable flexibility is displayed and that it is only reasonable to picture even cyclic constrained peptides as having numerous possible conformations.

Acknowledgment. We thank Prof. Victor J. Hruby and Dr. Fahad Al-Obeidi for numerous interesting discussions and the Robert A. Welch foundation and the National Institutes of Health for partial support. Finally we thank the San Diego Supercomputer Center for generous use of their Cray X-MP and Y-MP machines.

Registry No. DPDPE, 100111-01-1.